Molecular Biology of the Cell
Vol. 20, 1878–1889, March 15, 2009

Microtubule and Cell Contact Dependency of ER-bound PTP1B Localization in Growth Cones

Federico Fuentes and Carlos O. Arregui

Instituto de Investigaciones Biotecnológicas, Universidad de San Martín, 1650 San Martín, Buenos Aires, Argentina

Submitted July 2, 2008; Revised December 15, 2008; Accepted January 13, 2009
Monitoring Editor: Erika L. Holzbaur

PTP1B is an ER-bound protein tyrosine phosphatase implied in the regulation of cell adhesion. Here we investigated mechanisms involved in the positioning and dynamics of PTP1B in axonal growth cones and evaluated the role of this enzyme in axons. In growth cones, PTP1B consistently localizes in the central domain, and occasionally at the peripheral region and filopodia. Live imaging of GFP-PTP1B reveals dynamic excursions of fingerlike processes within the peripheral region and filopodia. PTP1B and GFP-PTP1B colocalize with ER markers and coalign with microtubules at the peripheral region and redistribute to the base of the growth cone after treatment with nocodazole, a condition that is reversible. Growth cone contact with cellular targets is accompanied by invasion of PTP1B and stable microtubules in the peripheral region aligned with the contact axis. Functional impairment of PTP1B causes retardation of axon elongation, as well as reduction of growth cone filopodia lifetime and Src activity. Our results highlight the role of microtubules and cell contacts in the positioning of ER-bound PTP1B to the peripheral region of growth cones, which may be required for the positive role of PTP1B in axon elongation, filopodia stabilization, and Src activity.

INTRODUCTION

Proper discrimination and response to extracellular signals by axonal growth cones are crucial for the wiring of the nervous system. The sensing activity is performed by receptors in the plasma membrane of growth cones, from which cell adhesion receptors represent a major category. In part, information relied by these receptors regulates the behavior of the cytoskeleton and other macromolecular complexes (Suter and Forscher, 2000; Huber *et al.*, 2003). Growth cone responses vary, but depend on the dynamic properties of microfilaments and microtubules. Microtubules explore dynamically the periphery of growth cones and occasionally penetrate into filopodia (Gordon-Weeks, 1991; Tanaka and Kirschner, 1991; Schaefer *et al.*, 2002; Brown and Bridgman, 2003; Schober *et al.*, 2007). It was early proposed that a subset of exploratory microtubules become selectively stabilized in response to extracellular cues (Kirschner and Mitchison, 1986; Mitchison and Kirschner, 1988). Indeed, imaging of Ti1 pioneer neurons in live grasshopper embryonic limb buds shows the selective invasion of microtubules toward growth cone branches that contact guidepost cells (Sabry *et al.*, 1991). Furthermore, studies in bag cell neurons of *Aplysia* show that microtubules quickly invade regions of contact between growth cone filopodia and neighboring cells or beads coated with ApCAM (Lin and Forscher, 1993; Suter *et al.*, 2004). This process would facilitate the translocation of vesicular and other membranous compartments to contact sites (Waterman-Storer *et al.*, 2000; Ligon and Holzbaur, 2007; Shaw *et al.*, 2007; Spiliotis *et al.*, 2008). Some degree of microtubule dynamics, however, seems to be required for events induced by target interactions of growth cones, including morphological changes, the assembly of an actin scaffold, and the activation of Src tyrosine kinases (Suter *et al.*, 2004; Wu *et al.*, 2008).

The endoplasmic reticulum (ER) is a continuous membranous compartment that essentially reaches every part of the cell (Vedrenne and Hauri, 2006). In growth cones the ER is prominent in the central domain and extends fingerlike processes dynamically to the peripheral region, which frequently coalign with microtubules (Dailey and Bridgman, 1989). These fingerlike processes are depleted by suppression of kinesin expression, implying they extend in association with microtubules (Feiguin *et al.*, 1994). In fact, dual fluorescence time-lapse analysis in living epithelial cells shows ER tubules extending to the cell periphery through mechanisms involving membrane sliding and binding to the microtubule tip attachment complex (Waterman-Storer and Salmon, 1998).

PTP1B was originally described as an ER-bound enzyme via a C-terminal targeting sequence (Frangioni *et al.*, 1992; Woodford-Thomas *et al.*, 1992). As the catalytic domain faces the cytosol, the enzyme has the potential for substrate dephosphorylation throughout the extensive branching network occupied by the ER. Indeed, BRET and FRET (bioluminescence and Förster resonance energy transfer, respectively), and BIFC (bimolecular fluorescence complementation) experiments show that ER-bound PTP1B interacts directly with, and dephosphorylates, cell surface receptors, either during their biosynthetic route to the cell surface, or after being endocytosed (Haj *et al.*, 2002; Boute *et al.*, 2003; Romsicki *et al.*, 2004; Anderie *et al.*, 2007). PTP1B is also associated with integrin and cadherin receptors in adhesion complexes (Balsamo *et al.*, 1996, 1998; Arregui *et al.*, 1998).

This article was published online ahead of print in *MBC in Press* (http://www.molbiolcell.org/cgi/doi/10.1091/mbc.E08–07–0675) on January 21, 2009.

Address correspondence to: Carlos O. Arregui (carregui@iib.unsam.edu.ar).

Abbreviations used: BIFC, bimolecular fluorescence complementation; BRET, bioluminiscence resonance energy transfer; FRET, fluorescence resonance energy transfer; RGC, retinal ganglion cell.

Interestingly, the accumulation of substrate trapping mutants of PTP1B at peripheral cell-matrix adhesions is blocked by nocodazole, suggesting that microtubules play a role in this process (Hernández *et al.*, 2006).

PTP1B mRNA is highly expressed in the pyramidal cell layer of the hippocampus (Guan *et al.*, 1990; Shifrin and Neel, 1993). PTP1B was also expressed in retina, and inhibition of the function or expression of PTP1B in dissociated retinal cells reduces N-cadherin– and β1-integrin–dependent neurite outgrowth on purified substrata (Balsamo *et al.*, 1996; Pathre *et al.*, 2001; Xu *et al.*, 2002). In the present article we investigated the distribution and dynamics of PTP1B in axonal growth cones. We found that PTP1B is bound to the ER, localizes prominently at the central domain of growth cones, and extends dynamically into the peripheral region, including filopodia. Both microtubule dynamics and cell contacts modulate this PTP1B distribution and dynamics. We also evaluated the function of PTP1B in axonal elongation and growth cone dynamics. We show that PTP1B is required for axon elongation and positively regulates the length and lifetime of growth cone filopodia. Finally, using a FRET reporter, we show that, at the growth cone, PTP1B is required for normal activation of Src.

MATERIALS AND METHODS

Materials

DMEM, neurobasal medium, F12, N2, B27, ITS, L-glutamine, gentamicin, penicillin-streptomycin, trypsin, fetal bovine serum, horse serum, and laminin were from Invitrogen (Carlsbad, CA). Poly-L-lysine and ovoalbumin were from Sigma-Aldrich (St. Louis, MO). Coverglasses were from Marienfeld (Lauda-Königshofen, Germany).

DNA Constructs

pEGFP-N1 and pDsRed2-C1 were from Clontech (Palo Alto, CA). Expression vectors encoding green fluorescent protein (GFP)- and hemagglutinin (HA)-tagged forms of wild-type PTP1B and the dominant-negative mutant PTP1B-C215S were previously described (Arregui *et al.*, 1998; Balsamo *et al.*, 1998). The pMT2-TC-PTP was kindly provided by Nick Tonks (Cold Spring Harbor Laboratory, NY). The plasmid encoding the membrane-targeted Src FRET reporter was a gift of Shu Chien (University of California at San Diego). The chicken c-Src Y527F (a gift of Kenneth Kaplan, University of California at Davis), and c-Src Y416F (provided by Jonathan Cooper, Fred Hutchinson Cancer Research Center, Seattle, WA) were subcloned into the EcoRI/BamHI and BamHI/HindIII sites of pcDNA3.1/zeo (Invitrogen), respectively. GFP-SERCA2a in pEGFP-N3 was a gift of Takafumi Inoue (University of Tokyo, Japan).

Antibodies

Two monoclonal antibodies against PTP1B, Ab-1, used at 1/200, and clone 15, used at 1/500, were from Calbiochem (EMD Biosciences, San Diego, CA) and BD Biosciences (Franklin Lakes, NJ), respectively. Rabbit polyclonal anti-PTP1B (used at 1/50) was from Upstate Biotechnology (Lake Placid, NY). Monoclonal anti-βIII-tubulin (TUJ1, used at 1/1000) was from Covance (Princeton, NJ). Monoclonal anti-tau-1 (used at 1/1000) was a gift from Lester Binder (Northwestern University, Chicago, IL). Monoclonal anti-tyrosinated tubulin and polyclonal anti-calnexin (both used at 1/1000) were from Sigma-Aldrich. Polyclonal anti-detyrosinated tubulin (used at 1/1000) was a gift from Dante Beltramo (Ceprocor, Córdoba, Argentina) and Carlos Arce (Universidad de Córdoba, Argentina; Arregui *et al.*, 1997). phalloidin-TRITC (used at 1/1000), phalloidin-AMCA (used at 1/200), and Alexa Fluor488- and Alexa Fluor546-conjugated secondary antibodies (both used at 1/500) were from Invitrogen.

Hippocampal Cultures

Hippocampal neuronal cultures were prepared from brains of 18-d-old rat fetuses as described in Goslin and Banker, 1991, with modifications. Briefly, tissue was treated with 0.25% trypsin in (HBSGK; 20 mM HEPES, 150 mM NaCl, 2 mM glucose, 3 mM KCl, pH 7.4) for 15 min at 37°C. A single-cell suspension was obtained in neurobasal medium containing 0.3 mg/ml glutamine, 100 U/ml penicillin, 100 μg/ml streptomycin, and 10% (vol/vol) horse serum. Cells were plated at desired concentrations (ranging from 5000 to 50,000 cells per cm^2) on coverglasses coated with 0.8 mg/ml poly-L-lysine prepared in borate buffer 0.1 M, pH 8.5. After 2 h in a 5% CO_2 humidified incubator (37°C), medium was changed to serum-free neurobasal medium, supplemented with 0.5 mg/ml ovalbumin, N2, and B27. Cells were maintained in incubator for 1–21 d before fixation and imaging.

Retina Cultures

Cultures of entire retinas were performed as previously described (Marrs *et al.*, 2006) with minor modifications. Eyes from 6-d-old chick embryos (E6) were dissected in HBSGK. Isolated retinas were mounted onto black filters (0.8-μm pore) of mixed cellulose esters (MF-Millipore; Millipore, Billerica, MA), with the vitreous side facing away from the filters. Flat-mounted retinas were cultured in regular tissue culture dishes in DMEM supplemented with 10% fetal bovine serum, 100 U/ml penicillin, and 100 μg/ml streptomycin in a 5% CO_2 humidified incubator (37°C) for 2 d. Cultures of dissociated retina cells were prepared from E6 chick retina as described previously (Arregui *et al.*, 2000). The cell suspension was plated on coverglasses coated with 0.25 mg/ml poly-L-lysine and 20 μg/μl laminin. Cells were maintained in F12 medium supplemented with 5 mM HEPES, pH 7.2, 0.6% glucose, 5 mg/ml gentamicin, 5 μg/ml insulin, 100 μg/ml transferrin, and 5 ng/ml sodium selenite.

Electroporation

Flat-mounted retinas were electroporated during the same day of preparation, using a square wave pulse electroporator with 1-cm diameter circular planar silver electrodes (LV-1.0 electroporator; EMSUR, Buenos Aires, Argentina). Filters with the retina facing up were placed over the anode. DNA (10 μg) diluted in 100 μl of cold F12 medium was overlaid onto the retina, and the cathode was set parallel to the anode at a distance of 2 mm. DNA was electroporated by two pulses of 50 V, each 20-ms duration, with a 1-s interval. Flat-mounted retinas were placed upside down on glass-bottom dishes. Electroporated retinas showing neurons with evidence of ill health, including beaded axons were discarded. Electroporation of hippocampal neurons in suspension (100 μl, ~10^6 cells) were performed with one 90 V pulse of 20-ms duration. Cells were immediately plated on rounded coverglasses for analysis as fixed cells or on glass-bottom 35-mm dishes (MatTek, Ashland, MA) for analysis by time lapse.

Immunofluorescence

Whole-mounted retinas and dispersed cells were fixed with 4% paraformaldehyde, 4% sucrose in PBS (137 mM NaCl, 2.7 mM KCl, 10 mM Na_2HPO_4, and 1.8 mM KH_2PO_4, pH 7.4) for 60 and 20 min, respectively. Then, samples were permeabilized with 0.5% Triton X-100 in PBS for 10 min (30 min for the whole mounts) at room temperature and blocked with 3% BSA in PBS overnight at 4°C. Incubations with the primary and secondary antibodies were carried out in a humid chamber for 1 h at 37°C. Samples were mounted in PBS/glycerol (1:1, vol/vol) and observed through a 100×/1.4 NA objective in a Nikon E600 microscope (Melville, NY) coupled to a Spot RT Slider CCD camera (Diagnostic Instruments, Sterling Heights, MI). Images were analyzed with the ImageJ software (http://rsb.info.nih.gov/ij/ NIH, Bethesda, MD).

Time-Lapse Imaging

Dissociated hippocampal neurons or flat-mounted retinas in glass-bottom dishes were placed on the stage of a Nikon TE2000 inverted microscope enclosed within an incubator system set at 37°C (Solent Scientific, Fareham, United Kingdom). Imaging medium was phenol red–free DMEM with high-glucose, supplemented with 4 mM L-glutamine and 25 mM HEPES buffer, 10% fetal bovine serum, and antibiotics. The medium also contained 0.5 U/ml oxyfluor (Oxyrase, Mansfield, OH) to prevent photobleaching and photodamage. Hippocampal neurons were imaged with a 60×/1.4 NA Plan Apo objective; whole mounted retinas were imaged with a 20×/0.4 NA Plan Fluor objective. The excitation light was attenuated using ND8 neutral density filters. Rapid switching of fluorescent wavelengths was accomplished by excitation and emission filter wheels (EGFP, excitation 470/20, emission 525/40; DsRed2, excitation 565/25, emission 620/60) used in combination with the 86007bs multiband dichroic mirror (Chroma Technology, Brattleboro, VT). Epifluorescence Smartshutter and filter wheels were controlled by the Lambda 10-B controller (Sutter Instrument, Novato, CA). Images were acquired with an Orca-AG cooled CCD camera (Hamamatsu Photonics, Hamamatsu, Japan) using 2 × 2 binning. Exposure times ranged from 0.05 to 0.20 s. Under our experimental conditions, no significant photobleaching was detected. All peripherals were controlled with Metamorph software (Molecular Devices, Downingtown, PA). Stacks of the image sequences were built using the Metamorph or the ImageJ software. For analysis of the GFP-PTP1B dynamics in growth cones of hippocampal neurons, consecutive images of the red and green channels were acquired every 10 s during 10 min. For quantification of intraretinal axonal elongation, images were acquired every 3 min for a total period of 45–60 min or every 30 min during 5 h. We did not notice signs of cell deterioration (blebs and loss of motility) under our experimental conditions.

Retrospective Immunofluorescence

To analyze events during the early phase of growth cone-target interactions, neurons with growth cones close (~20 μm) to neighboring growth cones were

identified and imaged by phase-contrast time-lapse analysis (images taken every 3–10 min) until a filopodium made a contact. Then, cells were immediately fixed and processed for immunofluorescence. The original contact region was identified and analyzed.

Nocodazole and Taxol Treatments

Stock solutions of nocodazole (50 mM) and taxol (12 mM) were prepared in DMSO. Drugs were diluted in serum-free medium and used in the range of 0.1–10 μM for nocodazole and 0.1–50 μM for taxol. Incubations were done at 37°C for 20 min, with the exceptions indicated. For nocodazole washout analysis, cells were washed three times with prewarmed HBSGK and then incubated with fresh medium for the times indicated. For time-lapse analysis, sets of four images of selected growth cones were acquired with a 2-min interval, before, during, and after nocodazole removal. Imaging during the nocodazole (50 nM) treatment started 5 min after addition of the drug. Imaging after the nocodazole removal started after a 20-min incubation with the fresh medium.

Quantitative Determinations

For quantitative analysis of PTP1B punctate in the peripheral domain of the growth cone (see Figure 3), paired two-color images for F-actin and PTP1B were acquired, adjusting the exposure times to obtain the maximal dynamic range without saturating the detector. The intensity of the fluorescence signals in the positive scores (PTP1B channel) was at least twice that of the surrounding area. A single value of threshold was established for each of the three independent experiments. F-actin images were used to create a mask delimiting the area of the peripheral domain of the growth cone, which was pasted on the corresponding thresholded PTP1B image. PTP1B punctate within the mask was counted, and values were expressed as punctate per 10 μm^2 of growth cone area. All image processing was performed using the ImageJ software. Data were analyzed by ANOVA and Bonferroni posttest, and differences were considered significant if $p < 0.05$.

Parameters of GFP-PTP1B dynamics in living hippocampal neurons were obtained from time-lapse series of images (taken every 10 s) of selected growth cones in apposition with other neurons (cell–cell contact condition) or totally free of cell–cell contacts. To determine the growth and retraction of GFP-PTP1B processes, the length of lines traced over the free trajectory of the processes was measured for each time point using Metamorph, and then data were transferred to Excel (Microsoft, Redmond, WA). Elongation/retraction rates were calculated from the slope of curves of length versus time representing the phases of net growth and retraction (with at least three consecutive intervals for each phase). To measure the filopodial lifespan, the period of time between the appearance and disappearance of DsRed extensions was recorded. The maximal length achieved by filopodia was also recorded.

To determine the retinal ganglion cell axon extension, background-subtracted DsRed images were thresholded and the position of the leading edge of the axon was plotted against time. Intervals with a net advance or retraction lower to 2 μm were considered as pauses. The values of velocities, and the periods of advances, pauses, and retractions were compared between retinas cotransfected with GFP-PTP1B-CS or the pEGFP-N1 vector. Statistical differences in Student's t test were considered significant if $p < 0.05$. The axonal length of cultured hippocampal neurons was measured after fixation and labeling with anti-Tau-1. The length of tau-positive processes was measured using the segmented lines menu of ImageJ.

FRET Imaging and Analysis

Hippocampal neurons were electroporated with a previously characterized membrane-targeted Src FRET probe (Wang *et al.,* 2005) together with either, HA-tagged wild-type PTP1B or the dominant-negative PTP1B C215S (Arregui *et al.,* 1998). In a few experiments, the FRET reporter was also cotransfected with the constitutively active form of c-Src-Y527F or the catalytically impaired c-Src-Y416F. Transfected cells were fixed 48 h later and analyzed with a Nikon TE2000 inverted microscope using a 60×/1.4 NA Plan Apo objective. Incident light was attenuated using ND8 neutral density filters. Filters used for dual-emission ratio imaging (enhanced cyan fluorescent protein [ECFP] excitation 430/25, ECFP emission 470/30; enhanced yellow fluorescent protein [EYFP] emission 535/30) were placed in filter wheels and combined with the dual dichroic mirror 86002v2bs (Chroma Technology). ECFP and EYFP images were acquired with an Orca-AG cooled CCD camera (Hamamatsu Photonics) using 4 × 4 binning and exposure times from 0.5 to 1 s. After background subtraction, ECFP/EYFP ratio images were generated and used to represent changes in the FRET efficiency. As previously reported, phosphorylation of the FRET reporter by Src, enhances the CFP emission at the expense of YFP emission (Wang *et al.,* 2005). Ratio values and intensities of YFP were used to generate images by intensity modulated display (Metamorph). For quantification of FRET changes, the average ECFP/EYFP ratios along line scans (1 pixel wide) traced over the entire set of filopodia for each growth was calculated using Excel.

RESULTS

Distribution of PTP1B in Hippocampal Neurons

Previous studies using nerve growth factor–differentiated PC12 cells and retinal neurons suggested that PTP1B is required for adhesion and neurite outgrowth (Pathre *et al.,* 2001; Xu *et al.,* 2002). However, a detailed study of the distribution of PTP1B in neurons was lacking so far. We have addressed this issue in well-characterized cultures of rat hippocampus, which consist in relatively homogeneous populations of neurons that differentiate axon and dendrites according to a stereotyped sequence of developmental events (Dotti *et al.,* 1988). Shortly after plating, neurons form a surrounding lamella (stage 1) that later is replaced by several short, minor processes (stage 2). The morphological polarization become evident when one of the minor processes overgrow the rest (stage 3), frequently depicting a large growth cone at the tip (Bradke and Dotti, 1997). Subsequently, the fast-growing process differentiates into the axon, and at later times, minor processes elongate and differentiate into dendrites (stage 4–5). We prepared cultures of hippocampal neurons representing each of the above developmental stages and analyzed, by immunofluorescence, the distribution of PTP1B. We obtained similar results with three different commercial antibodies. Under our experimental conditions the antibodies detect specifically PTP1B, being unable to recognize overexpressed TC-PTP, the closest homologue of PTP1B (Supplementary Figure S1). PTP1B exhibits a punctate distribution throughout all developmental stages. At stage 1, it is visible in the flat lamellar extensions surrounding the cell body and along the length of filopodia, including their tips (Figure 1A). At stage 2–3, PTP1B punctate extends into minor processes and the prospective axon, including its large growth cone (Figure 1B). At stage 4–5, a densely PTP1B punctate localizes along dendritic shafts and more sparsely into spines (Figure 1, C–E). PTP1B punctate was also evident in well-differentiated axons, as revealed by tau coimmunostaining (Figure 1E) and F-actin labeling (Figure 1D). In growth cones of stage 2–3 neurons the highest density of PTP1B punctate concentrates at the central domain; however, few scattered spots enter into the actin-rich, peripheral lamella, penetrating occasionally into filopodia (Figures 1, B and H, and 2A). A similar punctate distribution of PTP1B is observed in growth cones of embryonic chick retina neurons (not shown), suggesting that this distribution is not neuronal-type specific. We also analyzed the distribution of GFP-PTP1B. GFP added at the N-terminus does not affect the targeting of PTP1B (Arregui *et al.,* 1998; Balsamo *et al.,* 1998). The expression of GFP-PTP1B in hippocampal neurons does not affect the differentiation of axon and dendrites. In stage 3 neurons, GFP-PTP1B fluorescence is relatively uniform in minor processes and the axon, as revealed by tau immunolabeling (Figure 1G). In large growth cones of stage 2–3 neurons, fingerlike projections of GFP-PTP1B fluorescence emerge from the central domain, extending to the periphery and sometimes penetrating into filopodia, as revealed by DsRed cotransfection (Figure 1, I and J; Supplementary Movie S1). This distribution of GFP-PTP1B is similar to that described for DiOC6(3) staining (Dailey and Bridgman, 1989; Feiguin *et al.,* 1998). We were curious about the punctate distribution of the endogenous PTP1B, detected by immunolabeling. When we immunolabeled neurons after transfection with GFP-PTP1B, we observed a continuous distribution of the antibody label (not shown), suggesting that the punctate distribution of the endogenous PTP1B probably reflects its low concentration. PTP1B punctate does not colocalize with synapsin, synapto-

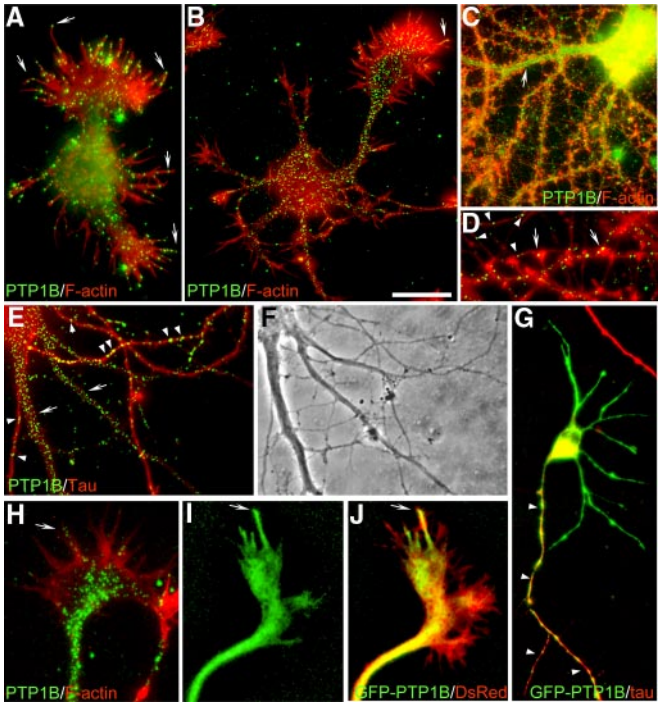

Figure 1. Distribution of PTP1B and GFP-PTP1B in hippocampal neurons. Dispersed hippocampal neurons were cultured for 24 h (A), 2 d (B and H–J), 6 d (G), and 22 d (C–F) in vitro. Cells were fixed and processed for immunofluorescence with anti-PTP1B (A–F and H) and anti-Tau1 (E–G). F-actin was detected by phalloidin-TRITC (A–D and H). GFP-PTP1B (G, I, J) and DsRed (J) were electroporated into cells in suspension before plating. Note that endogenous PTP1B is distributed in a punctate pattern at all developmental stages, in the axon (D, E, and G, arrowheads) and dendrites (C and E, arrows), including spines (D, arrows). In growth cones, PTP1B and GFP-PTP1B is prominent in the central domain (B and H) and in a variable manner in filopodia (A, B, and H–J, arrows). Bar, (A–C, E, and F) 15 μm; (D and H–J) 4 μm; (G) 20 μm.

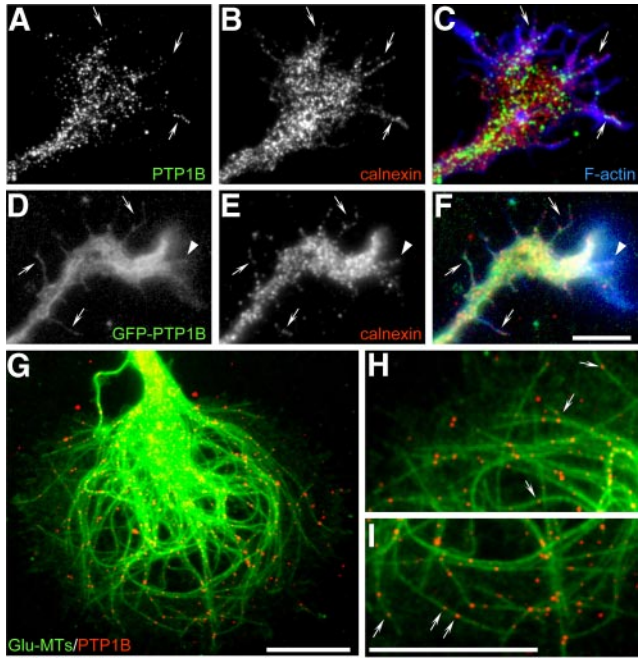

Figure 2. Colocalization of PTP1B and GFP-PTP1B with calnexin and microtubules. Stage 2–3 neurons were fixed and processed for immunofluorescence with anti-PTP1B (A and G–I), anti-calnexin (B and E), and anti-detyrosinated α-tubulin (Glu-MTs, G–I). F-actin was detected with phalloidin-AMCA (C and F). GFP-PTP1B was electroporated before plating (D). Note that endogenous PTP1B punctate and GFP-PTP1B codistributes with calnexin at the central region of growth cones and in filopodial extensions (arrows). Note also the codistribution of GFP-PTP1B projections with calnexin within the peripheral lamella (D–F, arrowheads). The endogenous PTP1B punctate coaligns with detyrosinated microtubules (G–I, arrows). Bars, 5 μm.

physin and cadherin along the neuronal processes, suggesting that is not present in transport vesicles (Supplementary Figure S2). Moreover, the fact that PTP1B punctate overlap with ER tubules in the peripheral, flat regions of nonneuronal cells present in the cultures suggest its ER localization (Supplementary Figure S2).

Association of PTP1B with the ER and Microtubules

In fibroblasts, PTP1B is bound to the cytosolic face of the ER (Frangioni *et al.,* 1992; Woodford-Thomas *et al.,* 1992; Balsamo *et al.,* 1998; Arregui *et al.,* 1998). In expanded lamella of large growth cones of hippocampal neurons the expression of GFP-PTP1B shows a reticular pattern resembling the ER (Figures 1I and 2D). To examine this further, we performed colocalization with calnexin and with the sarcoplasmic/endoplasmic reticulum calcium-ATPase (SERCA). Immunolabeling of calnexin shows a spotty distribution along the major neuronal compartments, including the growth cone (Figure 2B). This spotty distribution, by immunolabeling, was seen for several others ER markers, including calreticulin, SERCA, protein disulfide isomerase (PDI), and calnexin (Krijnse-Locker *et al.,* 1995; Bannai *et al.,* 2004; Willis *et al.,* 2005). PTP1B and calnexin punctate do not overlap; however, they codistribute at the expanded lamella of growth cones and filopodia (Figure 2, A–C). Similar codistribution is observed between calnexin and GFP-PTP1B (Figure 2, D–F) and between endogenous PTP1B punctate and transfected GFP-SERCA (not shown).

It was previously shown that DiOC6(3)-labeled ER tubules coalign with microtubules in the peripheral region of growth cones (Dailey and Bridgman, 1989). These ER tubules disappear from the peripheral region by suppression of kinesin expression (Feiguin *et al.,* 1994) suggesting that microtubules play a role in their localization. We analyzed the colocalization of PTP1B with microtubules in large growth cones of stage 2–3 hippocampal neurons. They display looped microtubules enriched in detyrosinated tubulin, which is a hallmark of stabilized microtubules (Kreis, 1987; Baas and Black, 1990; Arregui *et al.,* 1991). They also contain tyrosinated-rich microtubules, which are dynamic and usually project in a radial manner into the peripheral region (Figure 3K; Supplementary Figure S3; Arregui *et al.,* 1991; Dent and Gertler, 2003). PTP1B punctate coalign with both, detyrosinated and tyrosinated microtubules at the lamella of large growth cones (Figure 2, G–I; Supplementary Figure S3). This coalignment was also confirmed using GFP-PTP1B (Supplementary Figure S3). However, and as it was shown for DiOC6(3)-labeled ER (Dailey and Bridgman, 1989), not all GFP-PTP1B processes were associated with microtubules.

To determine the requirement of microtubules in the positioning of ER-bound PTP1B in growth cones, we analyzed neurons treated with nocodazole and taxol, drugs that impair the polymerization state and the distribution of microtubules. Incubation with nocodazole (100 nM, 20 min) leads to the simultaneous depletion of microtubules and the

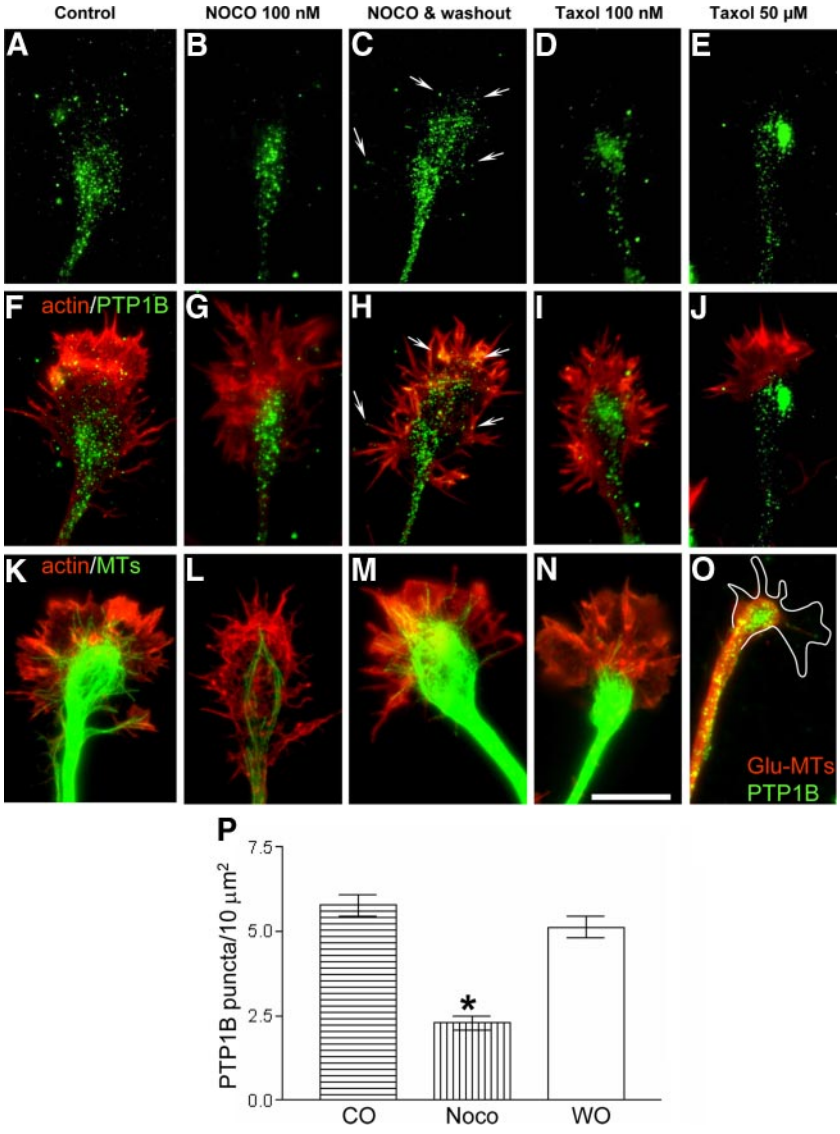

Figure 3. Redistribution of PTP1B and microtubules by nocodazole and taxol. Stage 2–3 hippocampal neurons were treated 20 min with nocodazol or taxol and then fixed and processed to detect PTP1B (A–J and O), microtubules (K–O), and F-actin (A–J). Note the redistribution of PTP1B punctate to the base of the growth cones after treatment with nocodazole (B, G, and P) and taxol (D, E, I, and J). By 120 min after nocodazole removal, PTP1B regain the distribution seen in the control, with some punctate at the peripheral region rich in F-actin (arrows, C, H, and P, compare with A). Tyrosinated microtubules, which invade the peripheral region of the growth cones in control condition (K), are depleted after treatment with nocodazole and taxol (L, N, and O). Removal of nocodazole allows for recovery of microtubules at the peripheral region (M). Incubation by 120 min with high concentrations of taxol leads to the accumulation of detyrosinated microtubules at the base of the growth cone, where they loop and surround the PTP1B punctate (O). Bars, 10 μm.

PTP1B punctate from the actin-rich peripheral region of growth cones (Figure 3, B, G, L, and P). PTP1B punctate collapses into a small area near the base of growth cones. Most likely, there is a redistribution of the PTP1B punctate because the washout of the nocodazole reverses the PTP1B and microtubule distribution to that found in control conditions (Figure 3, C, H, M, and P). Treatment with low concentrations of taxol (100 nM, 20 min) also leads to a depletion of microtubules and PTP1B from the peripheral region of the growth cone (Figure 3, D, I, and N). Higher concentration of taxol (50 μM, 120 min) leads to a concentration of PTP1B in large aggregates at the central domain (Figure 3, E and J). Under this condition tightly packed detyrosinated microtubules loop and surround the PTP1B aggregates (Figure 3O). Similar redistribution of calnexin was observed after treatment with nocodazole and taxol (not shown).

PTP1B Is Dynamically Positioned at the Periphery of Growth Cones and Filopodia in a Microtubule-dependent Manner

The variable presence of ER-bound PTP1B at the peripheral lamella and filopodia, and its redistribution after nocodazole and taxol, suggest that PTP1B is positioned dynamically at the periphery of growth cones and filopodia. To examine the dynamic behavior of PTP1B in growth cones, we coelectroporated GFP-PTP1B and DsRed in hippocampal neurons in suspension, and immediately plated at low density on glass-bottomed dishes. The growth cones of stage 2–3 neurons were analyzed by double fluorescence time-lapse studies. The DsRed fluorescence is used to track the full range of morphological changes of the growth cone. Most of the GFP-PTP1B fluorescence localizes at the central domain of the growth cone from which fingerlike processes emerge and extend in the peripheral region (Figure 4A). The emergence of these processes in a 10-min interval is 8.3 $\pm$ 1.4, and the average velocity of elongation and shortening is 3.9 $\pm$ 0.1 and 3.6 $\pm$ 0.1 μm/min, respectively (Table 1). Some GFP-PTP1B processes extend and penetrate into filopodia-like structures, (Figure 4A; Supplementary Movie S1). In growth cones showing a relatively persistent lamella, processes that reach the periphery are seen to curl and undergo a retrograde movement toward the central domain (Supplementary Movie S2).

We next tested whether microtubules are required for the dynamic projections of the GFP-PTP1B. After a brief treat-

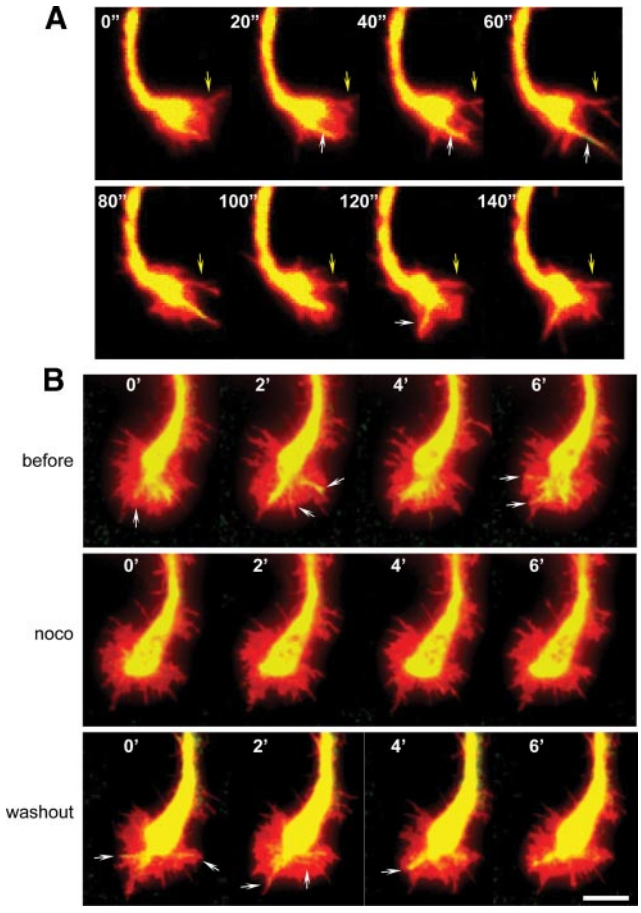

Figure 4. Dynamics of GFP-PTP1B projections and the effect of nocodazole. Hippocampal neurons were coelectroporated with GFP-PTP1B and DsRed in suspension and plated. Neurons at stage 2–3 were imaged every 10 s by time-lapse double fluorescence (in A, images every 20 s are showed). Note that not all filopodial extensions shown by DsRed contain GFP-PTP1B projections (A, yellow arrows). Fingerlike projections of GFP-PTP1B extend from the central region to the periphery and enter some filopodial-like structures (A, white arrows). In experiments with nocodazole and to minimize cell deterioration, series of four images were taken every 2 min before treatment, 5 min after starting the incubation with 50 nM nocodazole (noco), and 20 min after the washout of the drug (B). Note that dynamics of GFP-PTP1B projections seen before and after the washout (arrows) is abrogated during the period of incubation with nocodazole. Bar, 5 μm.

ment with nocodazole, growth cones retain the protrusive activity; however, in five independent experiments we never observed GFP-PTP1B processes emerging from the central domain and reaching the peripheral region (Figure 4B, noco). The washout of the drug, however, quickly rescued, in all cases, the emergence of dynamic projections of GFP-PTP1B that reach the peripheral region (Figure 4B, washout). These results were consistently repeated in five independent experiments.

Table 1. Parameters of GFP-PTP1B dynamics in the growth cone

	Contact free	Contact	p
Extension frequency[a]	8.3 ± 1.4 (12)	3.1 ± 1.0 (10)	<0.01
Retraction rate (μm/min)	3.8 ± 0.4 (13)	3.1 ± 0.2 (5)	NS
Elongation rate (μm/min)	4.9 ± 0.5 (16)	3.8 ± 0.5 (7)	NS

Values are the means ± SEM, with the number of cases analyzed in parentheses. NS, nonsignificant.

[a] The extension frequency was determined in a 10-min interval in growth cones that are totally isolated or growing in contact with a cell.

Cell–Cell Contacts Drive a Redistribution of PTP1B and Microtubules in Growth Cones

Studies in epithelial cells, and in growth cones of *Aplysia*'s bag neurons, showed that microtubules selectively stabilize at regions of cell–cell contacts (Waterman-Storer *et al.*, 2000; Ligon *et al.*, 2001; Ligon and Holzbaur, 2007; Suter and

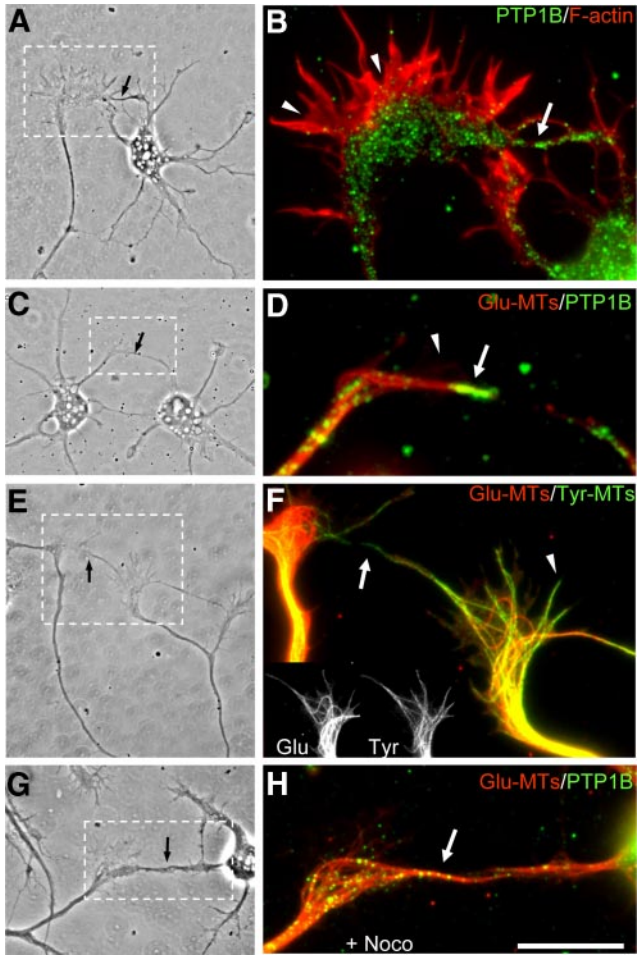

Figure 5. Distribution of PTP1B and microtubules in randomly occurring growth cone contacts. Hippocampal neurons were cultured until stage 2–3, at a density that allows frequent visualization of cell contacts. Cells were fixed and processed for detection of PTP1B (B, D, and H), F-actin (B), detyrosinated (Glu) microtubules (D, F, and H, red), and tyrosinated (Tyr) microtubules (F, green). The right panels are magnified views of contacting regions, framed in the phase-contrast images shown on the left (black arrows, A, C, E, and G). Note the selective enrichment of PTP1B punctate at the target-interaction axis of the growth cone (arrows in B and D, green label) compared with the scarce PTP1B punctate in the periphery of adjacent lamellar extensions (arrowheads in B and D). Microtubules at the contact region are enriched in detyrosinated tubulin (arrows in D and F). In contrast, microtubules at the noncontacting regions are enriched in tyrosinated tubulin (F, arrowhead). Detyrosinated microtubules and PTP1B punctate still remain aligned with the target-interaction axis after treatment with nocodazole (H, arrow). Bar, 10 μm.

Forscher, 2000). To examine the possibility that ER-bound PTP1B could be positioned at cell–cell contacts in a microtubule-dependent manner, we first analyzed the distribution of PTP1B in branches of growth cones that randomly established contacts with neighboring neurites and growth cones. In all cases analyzed, we found a selective enhancement of the PTP1B punctate over the contact region (Figure 5, A–D). In noncontacting lamellar extensions of the same growth cones, however, most of the PTP1B punctate remains at the central domain, as described for fully isolated growth cones (Figure 5B; also compare with Figures 1, B and H, 3, A and F, and 6). Quantifications of the mean fluorescence intensity, in equivalent areas of contacting and noncontacting peripheral regions, reveal a ~60% increase of the PTP1B label in the former (n = 13). We evaluated for the presence of stable microtubules in the contact regions by staining for detyrosinated tubulin. Indeed, microtubules aligned with the target-interaction axis are enriched in detyrosinated tubulin (Figure 5, D–F). In contrast, microtubules oriented to the peripheral region of noncontacting lamella of the same growth cones are enriched in tyrosinated tubulin (Figure 5F). To further confirm the selective coexistence of stable microtubules and PTP1B in the target-interaction axis, we incubated cells with nocodazole. In all cases analyzed a strong label of detyrosinated microtubules and PTP1B punctate remains aligned with the target-interaction axis after nocodazole treatment, whereas essentially no microtubules and PTP1B are found at adjacent noncontacting lamella (Figure 5, G, and H; see also Figure 3). Quantification of the mean fluorescence intensity of the PTP1B label show a ~70% increase in the contacting region respect to the noncontacting lamella (n = 13). To further evaluate these events at early phases of contact formation, we identified, in living neurons, growth cones that were near to adjacent growth cones or neurites and followed the behavior by phase-contrast time-lapse analysis until a filopodium established a contact. Within a time frame of 3–10 min after the contact, cells were fixed and processed for fluorescence detection of F-actin, PTP1B, β-catenin, and microtubules. In all cases (n = 5), there was an enhancement of PTP1B and detyrosinated tubulin associated with the contact area, particularly aligned with the target-interaction axis (Figure 6). F-actin and β-catenin also are abundant in this contact region. Incubation with nocodazole did not affect the distribution of PTP1B and detyrosinated microtubules in the target-interaction axis (Figure 6, nocodazole treatment). Collectively, these results are consistent with previous studies in epithelial cells showing that nascent cadherin-based cell–cell junctions tether and stabilize cortical microtubules (Waterman-Storer *et al.*, 2000).

The enhanced PTP1B punctate distribution in the growth cone periphery after cell targeting might be a consequence of the stabilization of the ER in the contact region. Indeed, time-lapse analyses of GFP-PTP1B in growth cones that have part of the membrane in contact with adjacent neurites reveal little activity of extension and retraction of fluorescent projections Figure 7 and Table 1; Supplementary Movie S2). In contrast, in areas where the membrane is not in contact there is high activity of extensions and retractions of GFP-PTP1B (Figure 7 and Table 1; Supplementary Movie S2).

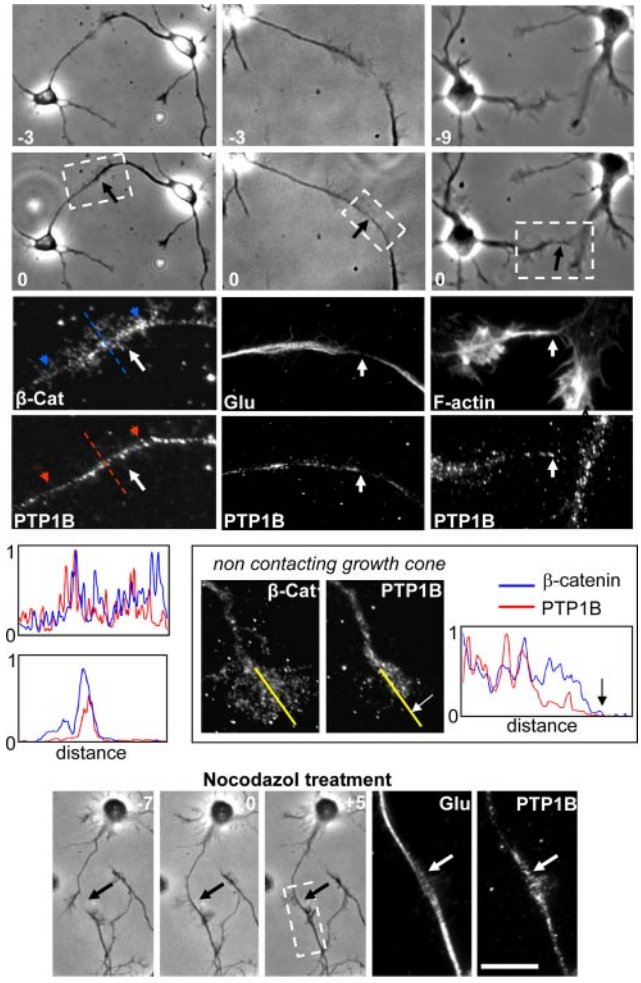

Figure 6. Distribution of PTP1B and cytoskeletal components during initial phases of growth cone-target contacts. Hippocampal neurons of stage 2–3 were monitored by phase-contrast time-lapse analysis until a growth cone filopodium made a contact with an adjacent growth cone (black arrows). Negative numbers indicate the time (minutes) previous to the contact (indicated by zero). Cells were immediately fixed and processed to detect PTP1B, F-actin, β-catenin, and detyrosinated (Glu) microtubules by fluorescence microscopy. Enlargements of the contact region (dashed boxes) reveal an invasion of PTP1B and detyrosinated (Glu) microtubules (white arrows) to this area. In noncontacting growth cones of the same culture, however, PTP1B remains more centrally located and did not invade the periphery. Profiles show pixel intensities of line scans for β-catenin (blue) and PTP1B (red) labels. Two profiles are shown from contacting growth cones. Top, line scans were taken longitudinally over the target-interaction axis, and the blue/red arrowheads mark the start (left) and the end (right) of the line scans. In the bottom profile, line scans were taken perpendicular to the contact axis (dashed lines). In the noncontacting growth cone, the position of the line scans is indicated by yellow lines, and the white and black arrows mark the border of the growth cone. Note the decrease of the PTP1B signal in the peripheral region compared with that of β-catenin. Also note that treatment with nocodazole (50 nM, 5 min) did not affect the contact and note the distribution of PTP1B and detyrosinated microtubules (bottom panels, arrows). Bar, 30 μm.

PTP1B Regulates Growth Cone Dynamics, and Src Activity

Recent work suggests that Src activity is required for filopodia initiation, extension, and dynamics (Robles *et al.*, 2005; Wu *et al.*, 2008). In addition, we and others have shown that Src activity is promoted by PTP1B in nonneuronal cells (Arregui *et al.*, 1998; Bjorge *et al.*, 2000). To gain insights into the function of PTP1B in growth cones, we determined the lifetime and length of filopodia in hippocampal neurons cotransfected with DsRed and GFP-PTP1B or GFP-PTP1B-CS. The PTP1B-CS is a catalytically inactive enzyme that binds to the substrate with similar affinity to the wild-type species (Xie *et al.*, 2002) and behaves as a dominant-negative

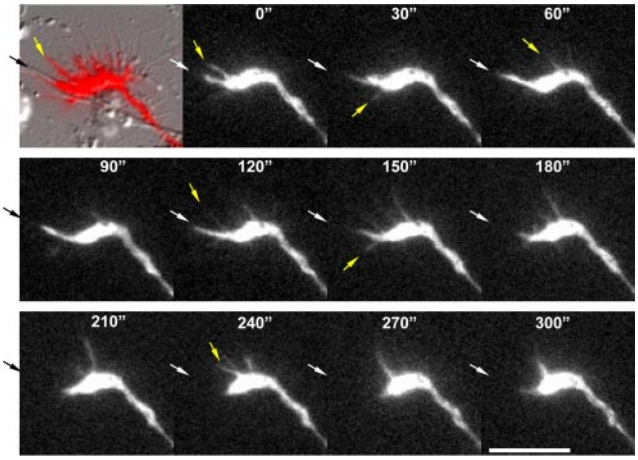

Figure 7. Dynamics of GFP-PTP1B projections in contacting and noncontacting regions of the growth cone. Hippocampal neurons of stage 2–3 were cotransfected with GFP-PTP1B and DsRed, and a growth cone partly in contact with a neurite was imaged by double fluorescence time-lapse analysis. The first image of the series was presented as an overlap of the DsRed fluorescence and the differential interference contrast image. For clarity, the subsequent images only depict the GFP-PTP1B fluorescence. Original images were acquired every 10 s, but here only frames obtained every 30 s are shown. Black arrow points the region of the growth cone that is in contact with the neurite. Note the low frequency of GFP-PTP1B extensions and retractions associated with the contact region (white arrows) in comparison to that in the noncontacting area (yellow arrows). Bar, 10 μm.

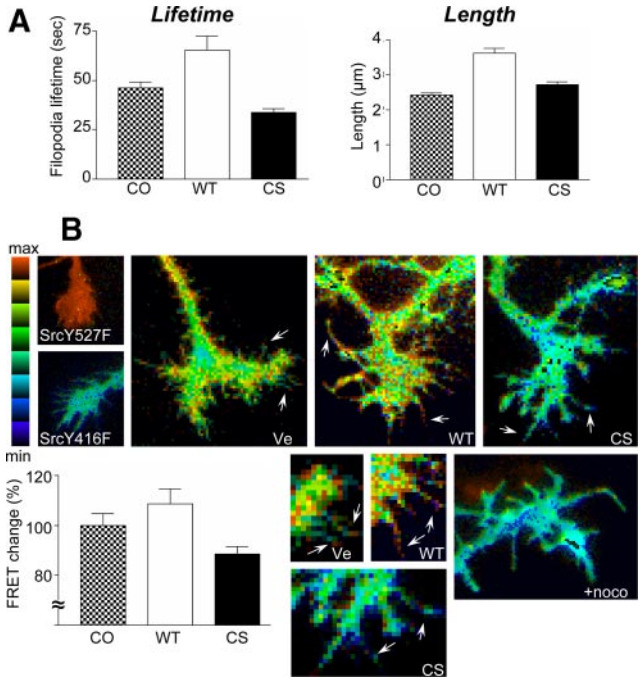

Figure 8. PTP1B regulation of filopodia dynamics and Src activity in growth cones. To analyze filopodia dynamics, hippocampal neurons were electroporated in suspension with DsRed and either GFP-PTP1B or GFP-PTP1B-CS. Cells were plated and developed to stage 2–3. Filopodia lifetime and maximal length were determined from the DsRed time-lapse images acquired every 10 s during 10 min (A). Values from five neurons (120-230 filopodia for each condition) were analyzed using one-way ANOVA with Dunnett's posttest. Note the opposite effect of overexpressing wild-type GFP-PTP1B or the dominant-negative GFP-PTP1B-CS on the filopodial lifetime (A, left graph). Also note the increase of filopodial length by GFP-PTP1B overexpression (A, right graph). To determine Src activity, cells were electroporated with an Src FRET reporter plus the constructs indicated in the panels (B). The FRET efficiency was represented by the intensity modulated display mode. Note maximal activity of the FRET sensor in neurons expressing a constitutively active Src (c-Src-Y527F) and basal signal in neurons expressing a catalytically impaired kinase (c-Src-Y416F). In neurons expressing the vector alone (Ve), peaks of FRET signal (yellow-red pixels) are concentrated near the margins of the growth cone, including the tips of filopodia (arrows). The signal is significantly increased and decreased by coexpression with wild-type PTP1B (WT) or the dominant-negative mutant PTP1B-CS (CS), respectively. Enlargements for each condition show the changes in the FRET signal in filopodia (arrows). The percentage of FRET change was calculated from line scans drawn over filopodia and shown in the bar graph. A brief treatment with nocodazole (100 nM, 20 min) abrogates the FRET signal (+noco). In the IMDs the ratio range was 0.4–0.85 except for Ve, which was 0.2–1.2.

mutant (Arregui *et al.*, 1998; Balsamo *et al.*, 1998; Rhee *et al.*, 2001). The expression of the GFP-PTP1B increases the filopodia lifetime by 40% respect to the control (Figure 8A, $p < 0.001$, one-way ANOVA with Dunnett's posttest). In contrast, the expression of GFP-PTP1B-CS decreased the filopodia lifetime by 27% respect to the control (Figure 8A, $p < 0.05$). The expression of the GFP-PTP1B also leads to a 50% increase of the length of filopodia (Figure 8A, $p < 0.001$). However, the expression of the GFP-PTP1B-CS also leads to a modest (13%) increase (Figure 8A, $p < 0.05$).

To determine the spatial variations of Src activity in growth cones, we transfected neurons with a previously characterized single-chain, membrane-targeted FRET reporter (Wang *et al.*, 2005). Briefly, this probe consists of the SH2 domain of c-Src separated by a flexible linker from a Src substrate peptide derived from p130Cas, both bracketed by ECFP and EYFP. As pointed out in the article of Wang *et al.* (2005), the proximity of the N- and C-terminals of the SH2 domain allows for a strong FRET signal in the absence of Src activity, which decreases upon Src activation and phosphorylation of the substrate. The pixel-by-pixel FRET signal can be represented as CFP/YFP ratio images and graphically visualized by the intensity-modulated display mode (Tsien and Harootunian, 1990). Thus, the spatial variations of Src activity can be easily appreciated in a 2D map. The coexpression of the FRET sensor with c-Src-Y527F, a constitutively active c-Src mutant, leads to a strong FRET signal throughout the growth cone (Figure 8B). In contrast, the coexpression with c-Src Y416F, a mutant with impaired catalytic activity, leads to a basal response of the FRET reporter (Figure 8B). The FRET change between the minimum and maximum response is ~30%, similar to that found in previous work (Wang *et al.*, 2005). Coexpression of the sensor with an empty vector shows peaks of FRET signal near the margins of the growth cone, including filopodial tips (Figure 8B). Coexpression with a plasmid carrying the wild-type PTP1B cDNA leads to an increase of the FRET signal, with peaks uniformly scattered in the lamella of the growth cone and filopodia (Figure 8B). In contrast, coexpression with the dominant-negative mutant PTP1B-CS leads to an overall reduction of the FRET signal to background levels (Figure 8B). Averaging FRET signals reveals that the FRET change between growth cones expressing the wild-type PTP1B and PTP1B-CS is ~20% (Figure 8B, bar graph).

In Figures 3 and 4 we showed that incubation with nocodazole abrogates the positioning of PTP1B and GFP-PTP1B at the peripheral region of growth cones. Thus, we examined the FRET signal in growth cones of neurons after a brief incubation

with nocodazole (100 nM, 20 min). This treatment leads to a reduction of the FRET signal to background levels, similar to the effect of overexpressing PTP1B-CS (Figure 8B).

Role of PTP1B in Axonal Extension

Results of the precedent section suggest that PTP1B regulates dynamic and fast morphological changes in growth cones. To determine the impact of impairing the function of PTP1B in the elongation of axons, a developmental process occurring in longer time frames, we compared the length of axons among hippocampal neurons expressing GFP-PTP1B and the GFP-PTP1B-CS. The length of axons in neurons expressing GFP-PTP1B does not differ significantly from that in nontransfected neurons of the same culture (Supplementary Figure S4). In contrast, the length of axons expressing the GFP-PTP1B-CS is about half of that in nontransfected neurons (nontransfected: 173.3 μm, GFP-PTP1B-CS: 85.7 μm, $p < 0.01$, one-way ANOVA with Dunnett's posttest; Supplementary Figure S4).

Previous work showed that PTP1B can associate with the N-cadherin complexes, and perturbing this association or blocking the PTP1B expression, impairs the adhesion and the neurite outgrowth of dissociated retina cells plated on purified laminin and N-cadherin substrata (Balsamo *et al.*, 1996; Pathre *et al.*, 2001; Xu *et al.*, 2002). In contrast to the simple and well-defined in vitro conditions, axons growing in developing tissues interact with a complex and variable environment. To determine the role of PTP1B in the elongation of intraretinal axons, we chose as a model system the retinal ganglion cells (RGCs) of the embryonic chick retina. The axons of these neurons run superficially on the vitreal side of the neural retina and are accessible for genetic manipulation when exposed to the culture medium in whole-mounted retinas (Figure 9A; Marrs *et al.*, 2006). We dissected entire chick E6 retinas to examine the elongation of intraretinal axons from RGCs located at the peripheral retina. Retinas were coelectroporated with vectors encoding the DsRed (Figure 9A) and the GFP, GFP-PTP1B wild type (Figure 9A), or the dominant-negative GFP-PTP1B-CS. Then transfected retinas were analyzed by double fluorescence time-lapse series. Determination of the overall axonal elongation rate measured during a 5-h period reveals that axons expressing the GFP-PTP1B-CS elongate significantly slower than axons expressing the GFP (25.5 $\pm$ 5 vs. 51.9 $\pm$ 7 μm/h, respectively, n = 8; Figure 9A). The growth cones alternate phases of advance, pause, and occasionally retract (Figure 9B; see also Zelina *et al.*, 2005). Because the overall axonal elongation rate does not provide information about which of the above phases are affected by the expression of GFP-PTP1B-CS, we performed time-lapse analyses during short periods (45–60 min) to assess the time that the growth cone spends in each of the three phases. Axons expressing the GFP-PTP1B-CS spend significantly less time in advance phases and correspondingly more time in pauses, in comparison to axons expressing the GFP (Figure 9, B and C). Moreover, the speed during the phase of advance in axons expressing the GFP and the GFP-PTP1B-CS is similar (118 $\pm$ 4 μm/h, n = 25, vs. 123 $\pm$ 5 μm/h, n = 31, respectively). These results indicate that changes in the duration of the growth and pause phases and not in the speed of advance are responsible for the slower elongation rate of RGC axons expressing the PTP1B-CS. In a similar kind of analysis, we did not find significant differences in the elongation rate and phase duration between axons expressing the GFP-PTP1B and the GFP control (not shown).

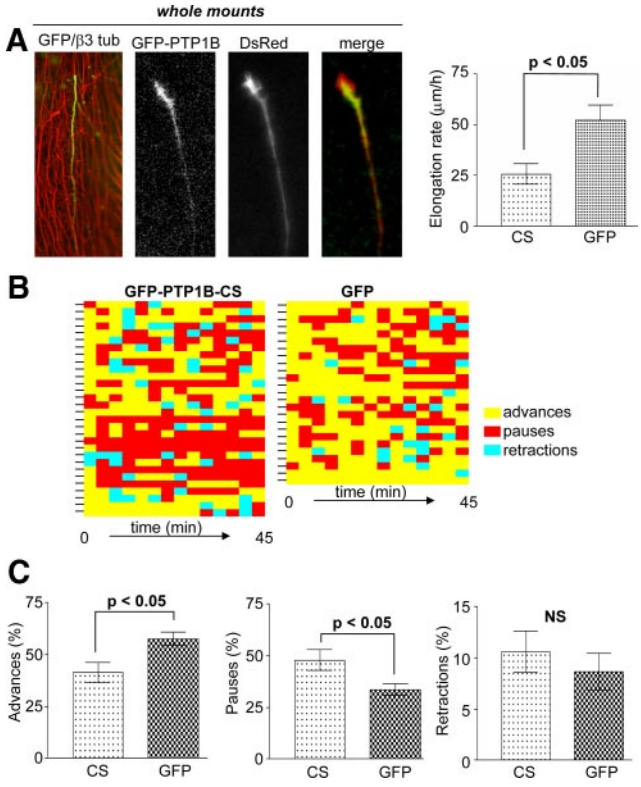

Figure 9. Role of PTP1B in intraretinal axon elongation. Whole-mounted retinas from E6 chick embryos were electroporated with DsRed and GFP, GFP-PTP1B, or GFP-PTP1B-CS. (A) Left panel, a typical intraretinal axon from ganglion cells expressing GFP and growing along tracks of preexistent axons, revealed by anti-β3-tubulin staining (red). Additional panels show an intraretinal growth cone coexpressing the DsRed and GFP-PTP1B. A graph representing the overall axonal elongation rates is shown at the right (n = 8, Student's *t* test, $p < 0.05$). Growth cones elongate alternating phases of advance, pauses, and occasionally, retractions (B). For a visualization and comparison of the elongation histories of several individual axons, each indicated by a mark at the left of the horizontal bars, the different phases are shown in different colors. The minimum length of each block corresponds to the interval between successive images (3 min). Note the increase of pauses (red color) in growth cones expressing the GFP-PTP1B-CS. Quantification of the percentage of time that growth cones spend in each phase in the whole observation period (45–60 min) reveals that the expression of GFP-PTP1B-CS reduces the percentage of time in the phases of advance and increase that in the phases of pauses (C).

DISCUSSION

Localization and Dynamics of PTP1B in Hippocampal Neurons

Here we show that regardless of the use of different antibodies for detection, the endogenous PTP1B in hippocampal neurons distributes in a punctate pattern in the soma, axon, and dendrites. In growth cones, PTP1B punctate consistently localizes at the central domain and occasionally penetrates into the peripheral region and filopodia. In mature dendrites, PTP1B punctate are particularly dense at the shaft of major branches and occasionally are present in spines. This variable localization in filopodia and spines suggests that PTP1B localization in these sites is dynamic. Indeed, time-lapse analysis of GFP-PTP1B supports this view. GFP-PTP1B shows a relatively uniform fluorescence in the processes and resembles the ER network in flat, thin regions. This distribu-

tion contrasts with the punctate pattern shown by immunolabeling the endogenous enzyme. Because similar distribution is observed when the transfected cells are immunolabeled, we presume that the punctate distribution of the endogenous PTP1B may reflect its low concentration and not an artifact of fixation.

In fibroblasts, PTP1B is associated to the cytosolic face of the ER membranes (Frangioni *et al.*, 1992; Woodford-Thomas *et al.*, 1992; Arregui *et al.*, 1998). The present studies in hippocampal neurons show that endogenous and transfected PTP1B colocalize with the ER markers calnexin and SERCA. PTP1B punctate did not colocalize with synapsin, synaptophysin, and cadherin along the neuronal processes, suggesting that is not present in transported vesicles. In addition, our time-lapse analyses of GFP-PTP1B never showed a mobile punctate fluorescence that could be attributed to a vesicular pool. Instead, GFP-PTP1B fluorescence in the flat central region of growth cones displays a reticular pattern, and the shape and dynamics of fingerlike projections of GFP-PTP1B extending to the peripheral region resemble that shown for the lipophilic dye DiOC6(3) in rat sympathetic neurons (Dailey and Bridgman, 1989). These observations argue that, in neurons, PTP1B is primarily an ER-associated enzyme. GFP-PTP1B, endogenous PTP1B, and calnexin, all undergo similar redistribution after treatment with nocodazole and taxol, further supporting this view. Our high-resolution dual fluorescence time-lapse studies reveal, for the first time, that ER-bound PTP1B is dynamically positioned at the peripheral region of the growth cone, entering in an apparently random manner, to some, but not all filopodia (Supplementary Movie S1).

Role of Microtubules in the Dynamic Positioning of PTP1B at the Growth Cone

Several findings indicate that ER-bound PTP1B is positioned dynamically to the peripheral region of growth cones in a microtubule-dependent manner. First, we show a significant coalignment of PTP1B and GFP-PTP1B with microtubules at the peripheral region of growth cones. Second, PTP1B and microtubules undergo similar redistributions after treatment with nocodazole and taxol, both being depleted from the peripheral region. Third, direct time-lapse observations show that dynamic projections of GFP-PTP1B to the peripheral region are reversibly abrogated by a brief treatment with nocodazole. Fourth, previous work shows that microtubules dynamically explore the periphery of the growth cone, with occasional penetration into filopodia (Arregui *et al.*, 1991; Gordon-Weeks, 1991; Sabry *et al.*, 1991; Schaefer *et al.*, 2002; Dent *et al.*, 2007). We found that PTP1B coaligns with tyrosinated microtubules, which represent a highly dynamic pool of microtubules extending in a radial manner to the peripheral region of growth cones. Fifth, we find that fingerlike projections of GFP-PTP1B extend toward the growth cone periphery at a speed of 4.9 ± 0.5 μm/min, which is similar to the elongation rates of ER tubules sliding on microtubules in the periphery of thin lamella of migrating newt lung epithelial cells (Waterman-Storer and Salmon, 1998). Collectively, these results highlight an active role of microtubules in the dynamic positioning of PTP1B at the growth cone periphery.

Growth Cone–Cell Contacts Influence PTP1B Distribution

In contrast to growth cones growing in isolation, microtubules and PTP1B punctate invade the peripheral region of growth cones, establishing contacts with cellular targets. This change in distribution of PTP1B and microtubules occurs selectively in the contact region because noncontacting lamella of the same growth cone displays only sparse PTP1B punctate and microtubules at the peripheral region. Furthermore, distribution of microtubules and PTP1B aligned along the target-interaction axis is not significantly affected by nocodazole, probably reflecting a selective tethering of microtubules in the cell-contacts axis (Sabry *et al.*, 1991; Waterman-Storer *et al.*, 2000; Ligon and Holzbaur, 2007; Shaw *et al.*, 2007). Indeed, we found an enrichment of detyrosinated tubulin, a hallmark of stable microtubules, selectively associated with the contact region. Time-lapse analysis of GFP-PTP1B in cones that are partly in contact with a cellular target shows frequent GFP-PTP1B projections in the noncontacting areas of the membrane but lower frequency of projections associated to the contacting area. Thus, our results suggest that cell–cell contacts stabilize the positioning of ER-bound PTP1B to the growth cone periphery, likely by the tethering of microtubules.

Regulation of Filopodial Dynamics and Src Activation by PTP1B

The protein tyrosine kinase Src localizes in growth cones where appears to regulate the formation and extension of filopodia (Robles *et al.*, 2005; Wu *et al.*, 2008). PTP1B dephosphorylates the C-terminus regulatory site of c-Src leading to its activation (Arregui *et al.*, 1998; Bjorge *et al.*, 2000). Thus, the dynamic positioning of PTP1B at the peripheral region of growth cones may contribute to the activation of Src. Using a membrane-targeted FRET sensor, we found that Src is active at the growth cone and filopodia, in agreement with previous immunodetection of phospho-active forms of Src (Robles *et al.*, 2005; Wu *et al.*, 2008). Interestingly, overexpression of PTP1B increased the FRET signal in the peripheral region and filopodia. In contrast, expression of the dominant-negative PTP1B-CS produced an overall decrease of the FRET signal. These results indicate that Src activity in the growth cone periphery and filopodia is modulated by PTP1B. In support to this view, a brief treatment with nocodazole, which depleted PTP1B from the peripheral region (Figures 3 and 4), also reduced the FRET signal in growth cone lamella and filopodia. Thus, PTP1B may be upstream in the chain of events activating Src in the peripheral region of growth cones and filopodia. As reported for Src (Robles *et al.*, 2005; Wu *et al.*, 2008), we found that overexpressing GFP-PTP1B leads to an increase of the lifetimes and length of filopodia. In contrast, the expression of the dominant-negative GFP-PTP1B-CS reduced filopodial lifetimes. Surprisingly, we did not find a decrease in the length of filopodia in growth cones expressing the GFP-PTP1B-CS. We do not have a clear interpretation for this result, but it may reflect compensatory effects by other phosphatases. The effect of the dominant-mutant on filopodial lifetimes, however, indicates that PTP1B play unique roles in their regulation. Filopodial lifetimes had been directly correlated with the levels of adhesion to the substratum (Bray and Chapman, 1985), and are also positively modulated by calcium signals that activate calpains (Robles *et al.*, 2003). The activation of a signaling pathway involving calpain-2, PTP1B, and c-Src was recently proposed for the regulation of invadopodia dynamics during cancer cell invasion (Cortesio *et al.*, 2008). Thus, we can envisage a scenario in which adhesive contacts made by filopodia activate a calpain-PTP1B-Src–signaling pathway that ultimately regulates filopodial motility.

Role of PTP1B in Axon Elongation

Here we tested the role of PTP1B in the axon elongation of embryonic chick RGCs in the complexity of the in situ 3D environment. We chose RGCs because their axons run superficially on the vitreal face of the neural retina and are

suitable for genetic manipulations and analysis in situ (Marrs *et al.*, 2006). We impaired the function of the endogenous PTP1B in a cell-autonomous manner by expression of the dominant-negative GFP-PTP1B-CS. We found that the elongation rate of RGC axons expressing the GFP-PTP1B-CS is reduced compared with that of neurons expressing the GFP vector. This seems a consequence of a change of behavior of growth cones because there is a significant increase of the periods of pauses in comparison to controls. The overall speed during the phases of advance is not significantly affected by the expression of GFP-PTP1B-CS, suggesting that the polymerization of the cytoskeleton required for the growth cone advance is not the primary target of the PTP1B. Instead the increase of pauses is compatible with a positive role of PTP1B in stabilizing cytoskeletal–membrane interactions during the growth cone advance. At the molecular level the dominant-negative PTP1B-CS may impair the integrin- and cadherin-mediated contacts made by RGCs axons with basal lamina components and with other cells, respectively (Thanos and Mey, 2001). Two major antecedents support this view. First, we and others have demonstrated that PTP1B is required for proper functioning of both integrin and cadherin receptors (Arregui *et al.*, 2000; Lilien and Balsamo, 2005; Burridge *et al.*, 2006; Sallee *et al.*, 2006). Second, dominant-negative mutants of cadherin and integrin cause significant retardation of axon elongation in *Xenopus* RGCs (Lilienbaum *et al.*, 1995; Riehl *et al.*, 1996). Cadherin coupling to the cytoskeleton can be quickly impaired by changes in the phosphorylation state of β-catenin, which reduces its affinity for cadherin and for α-catenin (Roura *et al.*, 1999; Xu *et al.*, 2002; Lilien and Balsamo, 2005). A possibility is that through dephosphorylation of critical residues on β-catenin, PTP1B promotes the stability of the β-catenin–N-cadherin interaction, the coupling to the cytoskeleton, and adhesion (Lilien and Balsamo, 2005). Further research is needed to define further the molecular targets of PTP1B regulation, in both integrin and cadherin complexes at the growth cone.

ACKNOWLEDGMENTS

We gratefully acknowledge Lester Binder (Northwestern University, Chicago, IL) for the anti-tau-1 antibody, Dante Beltramo (CEPROCOR, Córdoba, Argentina) and Carlos Arce (Universidad de Córdoba, Argentina) for the serum anti-tyrosinated tubulin, Nick Tonks (Cold Spring Harbor Laboratory, NY) for the TC-PTP, and Takafumi Inoue (University of Tokyo, Japan) for the GFP-SERCA. We thank Marcela Brocco (Instituto de Investigaciones Biotecnológicas, San Martín) for her initial help in dissecting hippocampi. This work was supported by the Agencia para la Promoción Científica y Tecnológica (PICTs 13381, 31939) and the Consejo Nacional de Investigaciones Científicas y Técnicas (CONICET; PIP 5266) to C. O. A. Federico Fuentes is recipient of a predoctoral fellowship from the CONICET.

REFERENCES

Anderie, I., Schulz, I., and Schmid, A. (2007). Direct interaction between ER membrane-bound PTP1B and its plasma membrane-anchored targets. Cell. Signal. *19*, 582–592.

Arregui, C. O., Busciglio, J., Caceres, A., and Barra, H. S. (1991). Tyrosinated and detyrosinated microtubules in axonal processes of cerebellar macroneurons grown in culture. J. Neurosci. Res. *28*, 171–181.

Arregui, C. O., Mas, C. R., Argaraña, C. E., and Barra, H. S. (1997). Tubulin tyrosine ligase: protein and mRNA expression in developing rat skeletal muscle. Dev. Growth Differ. *39*, 167–178.

Arregui, C., Leung, T-C., Balsamo, J., and Lilien, J. (1998). Impaired integrin-mediated adhesion and signaling in fibroblasts expressing a dominant-negative mutant PTP1B. J. Cell Biol. *143*, 861–873.

Arregui, C. O., Balsamo, J., and Lilien, J. (2000). Regulation of signaling by protein-tyrosine phosphatases: potential roles in the nervous system. Neurochem. Res. *25*, 95–105.

Baas, P. W., and Black, M. M. (1990). Individual microtubules in the axon consist of domains that differ in both composition and stability. J. Cell Biol. *111*, 495–509.

Balsamo, J., Leung, T.-C., Ernst, H., Zanin, M.K.B., Hoffman, S., and Lilien, J. (1996). Regulated Binding of a PTP1B-like Phosphatase to N-Cadherin: control of cadherin-mediated adhesion by dephosphorylation of β-catenin. J. Cell Biol. *134*, 801–813.

Balsamo, J., Arregui, C. O., Leung T-C., and Lilien, J. (1998). The nonreceptor protein tyrosine phosphatase PTP1B binds to the cytoplasmic domain of N-cadherin and regulates the cadherin-actin linkage. J. Cell Biol. *143*, 523–532.

Bannai, H., Inoue, T., Nakayama, T., Hattori, M., and Mikoshiba, K. (2004). Kinesin dependent, rapid, bi-directional transport of ER sub-compartment in dendrites of hippocampal neurons. J. Cell Sci. *117*, 163–175.

Bjorge, J. D., Pang, A., and Fujita, D. J. (2000). Identification of protein tyrosine phosphatase 1B as the major tyrosine phosphatase activity capable of dephosphorylating and activating c-Src in several human breast cancer cell lines. J. Biol. Chem. *275*, 41439–41446.

Boute, N., Boubekeur, S., Lacasa, D., and Tarik, I. (2003). Dynamics of the interaction between the insulin receptor and protein-phosphatase 1B in living cells. EMBO Rep. *4*, 313–319.

Burridge, K., Sastry, S. K., and Sallee, J. L. (2006). Regulation of cell adhesion by protein-tyrosine phosphatases cell-matrix adhesion I. J. Biol. Chem. *281*, 15593–15596.

Bradke, F., and Dotti, C. G. (1997). Neuronal polarity: vectorial cytoplasmic flow precedes axon formation. Neuron *19*, 1175–1186.

Bray, D., and Chapman, K. (1985). Analysis of microspike movements on the neuronal growth cone. J. Neurosci. *5*, 3204–3213.

Brown, M. E., and Bridgman, P. C. (2003). Retrograde flow rate is increased in growth cones from myosin IIB knockout mice. J. Cell Sci. *116*, 1087–1094.

Cortesio, C. L., Chan, K. T., Perrin, B. J., Burton, N. O., Zhang, S., Zhang, Z.-Y., and Huttenlocher, A. (2008). Calpain 2 and PTP1B function in a novel pathway with Src to regulate invadopodia dynamics and breast cancer cell invasion. J. Cell Biol. *180*, 957–971.

Dailey, M. E., and Bridgman, P. C. (1989). Dynamics of the endoplasmic reticulum and other membranous organelles in growth cones of cultured neurons. J. Neurosci. *9*, 1897–1909.

Dent, E. W., and Gertler, F. B. (2003). Cytoskeletal dynamics and transport in growth cone motility and axon guidance. Neuron *40*, 209–227.

Dent, E. W., *et al.* (2007). Filopodia are required for cortical neurite initiation. Nat. Neurosci. *9*, 1347–1359.

Dotti, C. G., Sullivan, C. A., and Banker, G. A. (1988). The establishment of polarity by hippocampal neurons in culture. J. Neurosci. *8*, 1454–l488.

Frangioni, J. V., Beahm, P. H., Shifrin, V., Jost, C. A., and Neel, B. G. (1992). The nontransmembrane tyrosine phosphatase PTP-1B localizes to the endoplasmic reticulum via its 35 amino acid C-terminal sequence. Cell *68*, 545–560.

Feiguin, F., Ferreira, A., Kosik, K. S., and Caceres, A. (1994). Kinesin-mediated organelle translocation revealed by specific cellular manipulations. J. Cell Biol. *127*, 1021–1039.

Gordon-Weeks, P. R. (1991). Evidence for microtubule capture by filopodial actin filaments in growth cones. Neuroreport *2*, 573–576.

Goslin, K., and Banker, G. (1991). Rat hippocampal neurons in low-density culture. In: Culturing Nerve Cells, ed. G. Banker and K. Goslin, Cambridge: MIT Press, 251–281.

Guan, K., Haun, R. S., Watson, S. J., Geahlen, R. L., and Dixon, J. E. (1990). Cloning and expression of a protein-tyrosine-phosphatase Proc. Natl. Acad. Sci. USA *87*, 1501–1505.

Haj, F. G., Verveer, P. J., Squire, A., Neel, B. G., and Bastiaens, P. I. (2002). Imaging sites of receptor dephosphorylation by PTP1B on the surface of the endoplasmic reticulum. Science *295*, 1708–1711.

Hernández, M. V., Davies Sala, M. G., Balsamo, J., Lilien, J., and Arregui, C. O. (2006). Endoplasmic reticulum-bound PTP1B is targeted to newly forming cell-matrix adhesions. J. Cell Sci., *119*, 1233–1243.

Huber, A. B., Kolodkin, A. L., Ginty, D. D., and Cloutier, J. F. (2003). Signaling at the growth cone: Ligand-receptor complexes and the control of axon growth and guidance. Annu. Rev. Neurosci. *26*, 509–563.

Kirschner, M., and Mitchison, T. (1986). Beyond self-assembly: from microtubules to morphogenesis. Cell *45*, 329–342.

Kreis, T. E. (1987). Microtubules containing detyrosinated tubulin are less dynamic. EMBO J. *6*, 2597–2606.

Krijnse-Locker, J., Parton, R. G., Fuller, S. D., Griffiths, G., and Dotti, C. G. (1995). The organization of the endoplasmic reticulum and the intermediate

compartment in cultured rat hippocampal neurons. Mol. Biol. Cell *6*, 1315–1332.

Ligon, L. A., Karki, S., Tokito, M., and Holzbaur, E.L.F. (2001). Dynein binds to β-catenin and may tether microtubules at adherens junctions. Nat. Cell Biol. *3*, 913–917.

Ligon, L. A., and Holzbaur, E.L.F. (2007). Microtubules tethered at epithelial cell junctions by dynein facilitate efficient junction assembly. Traffic *8*, 808–819.

Lilien, J., and Balsamo, J. (2005). The regulation of cadherin-mediated adhesion by tyrosine phosphorylation/dephosphorylation of β-catenin. Curr. Opin. Cell Biol. *17*, 1–7.

Lilienbaum, A., Reszka, A. A., Horwitz, A. F., and Holt, C. E. (1995). Chimeric integrins expressed in retinal ganglion cells impair process outgrowth in vivo. Mol. Cell Neurosci. *6*, 139–152.

Marrs, G. S., Honda, T., Fuller, L., Thangavel, R., Balsamo, J., Lilien, J., Dailey, M. E., and Arregui, C. (2006). Dendritic arbors of developing retinal ganglion cells are stabilized by β1-integrins. Mol. Cell. Neurosci. *32*, 230–241.

Lin, C-H., and Forscher, P. (1993). Cytoskeletal remodeling during growth cone-target interactions. J. Cell Biol. *121*, 1369–1383.

Mitchison, T., and Kirschner, M. (1988). Cytoskeletal dynamics and nerve growth. Neuron *1*, 761–772.

Pathre, P., Arregui, C., Wampler, T., Kue, I., Leung, T-C., Lilien, J., and Balsamo, J. (2001). PTP1B regulates neurite extension mediated by cell-cell and cell-matrix adhesion molecules. J. Neurosci. Res. *63*, 143–150.

Rhee, J., Lilien, J., and Balsamo, J. (2001). Essential tyrosine residues for interaction of the non-receptor protein-tyrosine phosphatase PTP1B with N-cadherin. J. Biol. Chem. *276*, 6640–6644.

Riehl, R., Johnson, K., Bradley, R., Grunwald, G. B., Cornel, E., Lilienbaum, A., and Holt, C. E. (1996). Cadherin function is required for axon outgrowth in retinal ganglion cells in vivo. Neuron *17*, 979–990.

Robles, E., Huttenlocher, A., and Gomez, T. M. (2003). Filopodial calcium transients regulate growth cone motility and guidance through local activation of calpain. Neuron *38*, 597–609.

Robles, E., Woo, S., and Gomez, T. M. (2005). Src-dependent tyrosine phosphorylation at the tips of growth cone filopodia promotes extension. J. Neurosci. *25*, 7669–7681.

Romsicki, Y., Reece, M., Gauthier, J. Y., Asante-Appiah, E., and Kennedy, B. P. (2004). Protein tyrosine phosphatase-1B dephosphorylation of the insulin receptor occurs in a perinuclear endosome compartment in human embryonic kidney 293 cells. J. Biol. Chem. *279*, 12868–12875.

Roura, S., Miravet, S., Piedra, S., García de Herreros, A., and Duñach, M. (1999). Regulation of E-cadherin/catenin association by tyrosine phosphorylation. J. Biol. Chem. *274*, 36734–36740.

Sabry, J. H., O'Connor, T. P., Evans, L., Toroian-Raymond, A., Kirschner, M., and Bentley, D. (1991). Microtubule behavior during guidance of pioneer neuron growth cones in situ. J. Cell Biol. *115*, 381–395.

Sallee, J. L., Wittchen, E. S., and Burridge, K. (2006). Regulation of cell adhesion by protein-tyrosine phosphatases II. Cell-cell adhesion. J. Biol. Chem. *281*, 16189–16192.

Schaefer, A. W., Kabir, N., and Forscher, P. (2002). Filopodia and actin arcs guide the assembly and transport of two populations of microtubules with unique dynamic parameters in neuronal growth cones. J. Cell Biol. *158*, 139–152.

Schober, J. M., Komarova, Y. A., Chaga, O. Y., Akhmanova, A., and Borisy, G. G. (2007). Microtubule-targeting-dependent reorganization of filopodia. J. Cell Sci. *120*, 1235–1244.

Shifrin, V. I., and Neel, B. G. (1993). Growth factor-inducible alternative splicing of nontransmembrane phosphotyrosine phosphatase PTP-1B pre-mRNA. J. Biol. Chem. *268*, 25376–25384.

Suter, D. M., Errante, L. D., Belotserkovsky, V., and Forscher, P. (1998). The Ig superfamily cell adhesion molecule, apCAM, mediates growth cone steering by substrate—cytoskeletal coupling. J. Cell Biol. *141*, 227–240.

Spiliotis, E. T., Hunt, S. J., Hu, Q., Kinoshita, M., and Nelson, W. J. (2008). Epithelial polarity requires septin coupling of vesicle transport to polyglutamylated microtubules. J. Cell Biol. *180*, 295–303.

Suter, D. M., and Forscher, P. (2000). Substrate-cytoskeletal coupling as a mechanism for the regulation of growth cone motility and guidance. J. Neurobiol. *44*, 97–113.

Suter, D. M., Schaefer, A. W., and Forscher, P. (2004). Microtubule dynamics are necessary for Src family kinase-dependent growth cone steering. Curr. Biol. *14*, 1194–1199.

Tanaka, E. M., and Kirschner, M. W. (1991). Microtubule behavior in the growth cones of living neurons during axon elongation. J. Cell Biol. *115*, 245–363.

Thanos, S., and Mey, J. (2001). Development of the visual system of the chick. II. Mechanisms of axonal guidance. Brain Res. Rev. *35*, 205–245.

Tsien, R. Y., and Harootunian, A. T. (1990). Practical design imaging system criteria for a dynamic ratio imaging system. Cell Calcium *11*, 93–109.

Vedrenne, C., and Hauri, H. P. (2006). Morphogenesis of the endoplasmic reticulum: beyond active membrane expansion. Traffic *7*, 639–646.

Wang, Y., Botvinick, E. L., Zhao, Y., Berns, M. W., Usami, S., Tsien, R. Y., and Chien, S. (2005). Visualizing the mechanical activation of Src. Nature *434*, 1040–1045.

Waterman-Storer, C. M., and Salmon, E. D. (1998). Endoplasmic reticulum membrane tubules are distributed by microtubules in living cells using three distinct mechanisms. Curr. Biol. *8*, 798–806.

Waterman-Storer, C. M., Salmon, W. C., and Salmon, E. D. (2000). Feedback interactions between cell–cell adherens junctions and cytoskeletal dynamics in newt lung epithelial cells. Mol. Biol. Cell, *11*, 2471–2483.

Willis, D., Li, K., Zheng, J-Q., Chang, J. H., Smit, A., Kelly, T., Merianda, T. T., Sylvester, J., van Minnen, J., and Twiss, J. L. (2005). Differential transport and local translation of cytoskeletal, injury-response, and neurodegeneration protein mRNAs in axons. J. Neurosci. *26*, 778–791.

Woodford-Thomas, T. A., Rhodes, J. D., and Dixon, J. E. (1992). Expression of a protein tyrosine phosphatase in normal and v-srctransformed mouse 3T3 fibroblasts. J. Cell Biol. *117*, 401–414.

Wu, B., Decourt, B., Zabidi, M. A., Wuethrich, L. T., Kim, W. H., Zhou, Z., MacIsaac, K., and Suter, D. M. (2008). Microtubule-mediated Src tyrosine kinase trafficking in neuronal growth cones. Mol. Biol. Cell *20*, 4611–4627.

Xie, L., Zhang, Y.-L., and Zhang, Z.-Y. (2002). Design and characterization of an improved protein tyrosine phosphatase substrate-trapping mutant. Biochemistry *41*, 4032–4039.

Xu, G., Arregui, C., Lilien, J., and Balsamo, J. (2002). PTP1B modulates the association of β-catenin with N-cadherin through binding to an adjacent and partially overlapping target site. J. Biol. Chem. *277*, 49989–49997.

Zelina, P., Avci, H. X., Thelen, K., and Pollerberg, G. E. (2005). The cell adhesion molecule NrCAM is crucial for growth cone behaviour and pathfinding of retinal ganglion cell axons. Development *132*, 3609–3618.